Electrostatic Interactions between Charged Amino Acid Residues and the Bacteriochlorophyll Dimer in Reaction Centers from *Rhodobacter sphaeroides*†

J. C. Williams, A. L. M. Haffa, J. L. McCulley, N. W. Woodbury, and J. P. Allen*

Department of Chemistry and Biochemistry and Center for the Study of Early Events in Photosynthesis, Arizona State University, Tempe, Arizona 85287-1604

Received July 30, 2001; Revised Manuscript Received October 17, 2001

ABSTRACT: The extent of electrostatic contributions from the protein environment was assessed by the introduction of ionizable residues near the bacteriochlorophyll dimer in reaction centers from *Rhodobacter sphaeroides*. Two mutations at symmetry-related sites, M199 Asn to Asp and L170 Asn to Asp, resulted in a 48 and 44 mV lowering of the midpoint potential, respectively, compared to the wild type at pH 8, while a 75 mV decrease in the midpoint potential was observed for the mutation L168 His to Glu. The decrease relative to wild type was found to be approximately additive, up to 147 mV, for various combinations of the mutations. As the pH was lowered from 9.5 to 6.0, the relative decrease in the midpoint potential became smaller for each of these three mutations. Titration of the pH dependence of the change in midpoint potential of the M199 Asn to Asp mutant compared to wild type yielded a pK_a value of 7.9 and a change in midpoint potential from low to high pH of 59 mV. The major effect of the mutation on the midpoint potential of the dimer is interpreted as stemming from a negative charge on the residue. An average dielectric constant of approximately 20 was estimated for the local protein environment, consistent with a relatively hydrophobic environment for residue M199. The rate of charge recombination between the primary quinone acceptor and the bacteriochlorophyll dimer decreased in the M199 Asn to Asp mutant at high pH, reflecting the decrease in midpoint potential.

Charged amino acid residues that are buried in the interior of proteins may have a significant impact on the electrostatic fields within the protein. Unlike surface charges, which are generally thought to be highly screened and often play a role in docking sites but have little effect on the fields inside the protein, buried charges can influence both the energy and the protonation state of nearby groups. Electrostatic interactions become particularly pertinent for proteins involved in electron-transfer reactions. For example, a number of theoretical models using crystallographic data from photosynthetic reaction centers have indicated that charged residues play an important role in the stabilization of charge-separated states (*1*−*6*).

Cofactors of reaction centers from purple bacteria include a bacteriochlorophyll dimer, which is the initial electron donor, two bacteriochlorophyll monomers, two bacteriopheophytins, two quinones, and a non-heme iron, and among these, only the bacteriochlorophyll dimer has a midpoint potential that is easily determined experimentally. The dimer midpoint potential has been shown to be sensitive to alterations in nearby residues, including changes in specific interactions such as hydrogen bonds and ligation of the Mg atom (reviewed in *7*). If charged residues are introduced near the dimer, new electrostatic interactions should result, and several general predictions can be made for their impact on the midpoint potential of the bacteriochlorophyll dimer. First, a negatively charged residue would be expected to stabilize the oxidized dimer, and thus lower the midpoint potential, while a positively charged residue would be expected to increase the midpoint potential. Second, the effect on the midpoint potential should vary inversely with distance, if the dielectric constant is uniform. Third, an increase in the effective dielectric constant of the protein will result in an increase in screening of a point charge and thus reduce its effect on the midpoint potential. In addition, an electrostatic interaction can be most reliably attributed to a point charge due to an ionizable amino acid residue if the effect is dependent on pH (for example, *8*, *9*). This requires that the pK_a value of the amino acid residue lies within the range through which the protein can be titrated.

We have tested the influence of electrostatic interactions on the dimer by site-directed mutagenesis of the reaction center from *Rhodobacter sphaeroides*. Distance and hydrophobicity considerations constrained the positions where a charged residue could be effectively introduced near the dimer to several nearby amino acid residues, including Asn M199 (Figure 1). This residue is approximately 10 Å from the surface of the reaction center, and is located shortly before the start of the D transmembrane helix. The closest distance from the oxygen or nitrogen atoms of the side chain to the conjugated atoms of the dimer is approximately 8.5 Å, with an average distance to all of the conjugated atoms of both bacteriochlorophylls of the dimer of 13.5 Å. Aspartic acid, histidine, and phenylalanine were substituted for the aspar-

† This work was supported by the USDA (1999-01753 to J.C.W. and J.P.A.) and the NSF (MCB-9817388 to N.W.W.). A.L.M.H. was supported by a Graduate Research Training grant from the NSF (DGE-9553456).

* To whom correspondence should be addressed. E-mail: jallen@asu.edu; Phone: 480-965-8241; FAX: 480-965-2747.

10.1021/bi011574z CCC: $20.00
Published on Web 11/20/2001

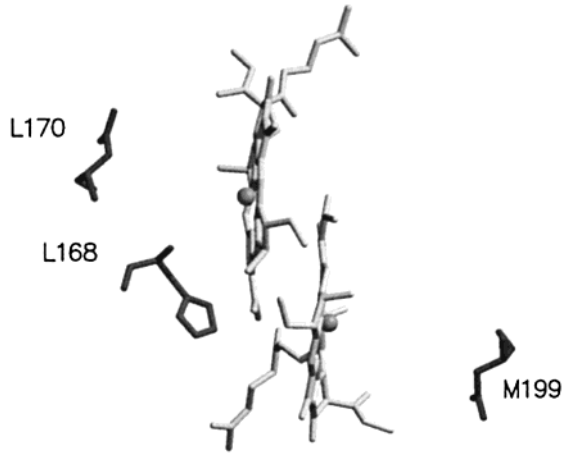

FIGURE 1: Structure of the reaction center from *Rhodobacter sphaeroides* showing bacteriochlorophyll dimer and residues Asn M199, Asn L170, and His L168. The view is down the approximate 2-fold symmetry axis of the protein.

agine residue at M199. Additional potentially negatively charged amino acid residues were introduced by the substitution of aspartic acid for asparagine at L170, the position on the L subunit that is symmetry-related to M199, and the substitution of glutamic acid for histidine at L168, which is hydrogen bonded to one of the acetyl substituents of the bacteriochlorophyll dimer. To investigate the additivity of these effects, three double combination mutants and a triple combination mutant were also constructed. In this study, we report the effects of these mutations on the energy of the bacteriochlorophyll dimer.

MATERIALS AND METHODS

Mutagenesis and Reaction Center Isolation. Mutations were made in the genes encoding the L and M subunits of the reaction center from *Rhodobacter sphaeroides* as previously described (*10*). A seven-residue histidine tag was added to the carboxy terminus of the M subunit of the wild type and all of the mutants except M199 Asn to Phe and M199 Asn to His (Haffa et al., manuscript in preparation). Reaction centers from the wild type and mutants containing changes at M199 were isolated as previously described (*10*), and His-tagged reaction centers were isolated following the protocol of Goldsmith and Boxer (*11*). For measurements in the pH range from 7.5 to 8.5, reaction centers were in 15 mM Tris-HCl, 0.01% Triton X-100, and 1 mM ethylenediaminetetraacetic acid (EDTA). The buffer was changed to 15 mM 2-(*N*-morpholine)ethanesulfonic acid (MES) for measurements from pH 6.0 to 7.0, and 15 mM 2-(cyclohexylamino)-ethanesulfonic acid (CHES) buffer was used for measurements from pH 9.0 to 9.5.

Titrations. Reaction center samples (A_{802}^{1cm} ~100) were adjusted to 60 mM KCl, and one or more of the mediators 2,3,5,6-tetramethyl-1,4-phenylenediamine (0.13 mM), potassium ferrocyanide (0.4 mM), potassium tetracyano-mono-(1,10-phenanthroline)-ferrate(II) tetrahydrate (0.15 mM), or dicyano-bis-(1,10-phenanthroline)-iron(II) dihydrate (0.4 mM) were added. Titrations were performed in a thin-layer electrochemical cell as previously described, using a Cary 5 spectrophotometer (Varian) to measure optical absorption spectra (*10*). After normalization of the spectra, the extent of reduction monitored at the maximum of the dimer Q_y transition was fit to the Nernst equation ($n = 1$).

Transient Optical Spectroscopy. A kinetic spectrophotometer of local design was used to measure the rate of charge recombination between the oxidized dimer and the reduced primary quinone (*12*). After addition of terbutryn (0.5 mM), reaction center samples (A_{802}^{1cm} ~1) were excited at 532 nm with the second harmonic of a Surelight Nd:YAG laser (Continuum) having a 5 ns pulse width, and the change in absorption of the Q_y transition at 865 nm was monitored. The data were fit to a single exponential with a second small component from a long-lived state.

Table 1: Changes in Midpoint Potential of the Mutants Relative to Wild Type

mutations	change in midpoint potential (mV)[a] pH 6.0	pH 8.0	pH 9.5
M199 Asn to His	0	4	9
M199 Asn to Phe	−1	1	6
M199 Asn to Asp	−20	−48	−73
L170 Asn to Asp	−24	−44	
L168 His to Glu	−48	−75	-88
L170 Asn to Asp + M199 Asn to Asp		−83	
L168 His to Glu + M199 Asn to Asp		−110	
L168 His to Glu + L170 Asn to Asp		−127	
L168 His to Glu + L170 Asn to Asp + M199 Asn to Asp		−147	

[a] Midpoint potential of mutant minus the midpoint potential of wild type at the pH indicated, with an estimated error of 5 mV.

RESULTS

Oxidation−Reduction Midpoint Potentials. The average value for the P/P^+ midpoint potential of the wild-type reaction center was 503 mV, in agreement with previous measurements (*10*). The error of the measurements was generally less than 5 mV as determined from multiple measurements. No significant difference was observed between the native and His-tagged versions of the wild type, as previously noted by Goldsmith and Boxer (*11*). The midpoint potentials at pH 8.0 were determined for the set of nine mutants, and the difference in the midpoint potential compared to wild type was calculated (Table 1). The midpoint potentials of the mutants with His or Phe substituted at M199 were very similar to that of wild type. The three mutants containing the single-site changes to acidic residues, M199 Asn to Asp, L170 Asn to Asp, and L168 His to Glu, all showed a decrease in the midpoint potential. The decreases for the M199 and L170 mutants were similar at 48 and 44 mV, respectively, and the decrease for the L168 mutation was slightly larger at 75 mV. The decrease in the midpoint potential for the L168 His to Glu mutant was similar to that seen previously for a His to Phe mutation at this site (*10*, *13*). The changes in midpoint potential for the double mutants were larger than for the single mutants, ranging from 83 to 127 mV, and the triple mutant had the largest decrease in midpoint potential of 147 mV.

The midpoint potential of the wild type decreased upon raising the pH, from an average of 518 mV at pH 6.0 to 498 mV at pH 9.5, as has been reported previously (*14*, *15*). The

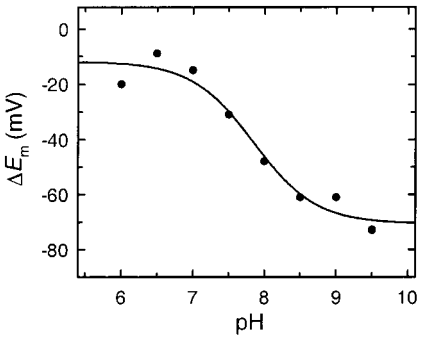

FIGURE 2: Difference in midpoint potential (ΔE_m) between the M199 Asn to Asp mutant and the wild type measured at particular pH values. The line is a fit of the data using the Henderson−Hasselbalch equation with a pK_a of 7.9.

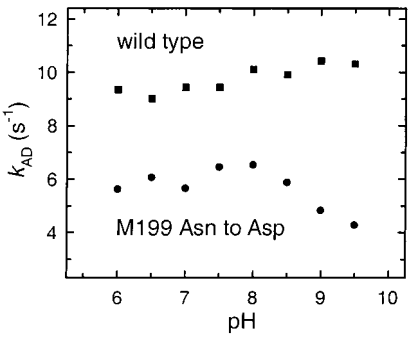

FIGURE 3: Charge recombination rate between the primary quinone and bacteriochlorophyll dimer (k_{AD}) as a function of pH for wild type and the M199 Asn to Asp mutant. Note the decrease in the rate with increasing pH for the mutant (circles) compared to the increase in rate for wild type (squares).

mutants with the Asn to His and Asn to Phe changes at M199 behaved similarly. The M199 Asn to Asp mutant showed a remarkable deviation from this pattern, resulting in a much larger difference from wild type at high pH than at low pH. The midpoint potential of this mutant was 20 mV below the midpoint potential of the wild type measured at pH 6.0, 48 mV below the wild type at pH 8.0, and 73 mV below the wild type at pH 9.5. The midpoint potential of the L170 Asn to Asp mutant similarly showed a smaller difference of 24 mV below the midpoint potential of the wild type at pH 6.0 compared to 44 mV below the wild type at pH 8.0, but the value at high pH could not be determined due to degradation of the sample. The L168 His to Glu mutant also showed a significant difference at low and high pH in the change in midpoint potential compared to the wild type at the same pH value.

The difference in the midpoint potential between the wild type and the M199 Asn to Asp mutant was determined at every 0.5 pH unit between pH 6.0 and 9.5 (Figure 2). These points were fit to the Henderson−Hasselbalch equation, yielding a pK_a value of 7.9 and a difference between the end points at low and high pH of 59 mV.

Charge Recombination Rate. Wild-type reaction centers have a charge recombination rate at pH 8 of approximately 10 s^{-1} that slightly increases with increasing pH (*16*). Measurements of the charge recombination rate in the wild-type reaction centers agreed with previous determinations. For the M199 Asn to Asp mutant, at values below pH 8, the charge recombination rate showed a trend similar to wild type, but with a slower rate of approximately 6 s^{-1}. Above pH 8, the charge recombination in this mutant deviated markedly from this trend, decreasing sharply until the rate was approximately 4 s^{-1}, or less than half that of wild type (Figure 3).

DISCUSSION

The oxidation−reduction midpoint potential of the bacteriochlorophyll dimer in the reaction center from *R. sphaeroides* was used as a probe for the electrostatic interaction of the dimer with nearby residues. Ionizable residues were introduced by mutagenesis, and the difference in the midpoint potential between the mutant and wild type at different pH values were determined. At residue M199, substitution of Phe or His for Asn resulted in very little change in the midpoint potential at any pH, while substitution of Asp resulted in a highly pH-dependent decrease in the midpoint potential relative to wild type. These results suggest that His at M199 is not ionized between pH 6.0 and 9.5, while Asp at this position becomes ionized at high pH, and that the major effect of the mutation on the midpoint potential of the dimer stems from a negative charge on the residue. A comparable change in midpoint potential was found when Asp was substituted for Asn at the symmetry-related position L170. The change at L168 due to the His to Glu substitution is complicated by the presence of the hydrogen bond between His L168 and the 3-acetyl group of the dimer (*17*). The similar decrease of 80 mV in the midpoint potential at pH 8 observed for the mutation L168 His to Phe (*10*) suggests that a significant contribution to changes in midpoint potential in reaction centers with alterations of this residue arises from the loss of the hydrogen bond between L168 His and the bacteriochlorophyll dimer.

For the M199 Asn to Asp mutant, titration of the change in midpoint potential yielded results that fit well to the Henderson−Hasselbalch equation, indicating a change in protonation state of the residue between low and high pH. The fit shows that the titration is essentially complete between pH 6.0 and pH 9.5 (Figure 2). At low pH, where the aspartic acid residue at M199 is assumed to be protonated, the midpoint potential of the mutant is nearly the same as wild type. At higher pH, the residue should acquire a negative charge as it becomes deprotonated. The negative charge on the residue would stabilize the positively charged oxidized dimer, resulting in a lowering of the midpoint potential, as is observed. This description assumes that the mutation introduces negligible changes in the electrostatic contributions of other residues.

The titration of the aspartic acid residue at M199 yields a fitted pK_a value of approximately 8, which is much higher than the pK_a of aspartic acid in solution. Shifts of pK_a values of amino acid side chains are well documented in a number of proteins (*18*, *19*). For example a glutamic acid introduced in staphyloccocal nuclease and an aspartic acid in thioredoxin have measured pK_a values of 7−9 (*20*, *21*). Such a shift in pK_a is generally explained as being due to the hydrophobic nature of the protein interior. The identity of residues near Asn M199 indicates that the position is fairly hydrophobic (Figure 4). The nearest residues are Ser M287 and Trp M294, which appear to form hydrogen bonds with Asn M199 in the wild-type structure. Residues Pro M200, Phe M201, and Gly M283 are also within 4.5 Å of the side chain of Asn M199. The hydrophobicity of the microenvironment near

FIGURE 4: Microenvironment of residue M199. Shown are Asn M199 and the surrounding amino acid residues, Pro M200, Phe M201, Gly M283, Ser M287, and Trp M294.

M199 was evaluated by calculating the fragmental hydrophobic constant (*22*), and a moderately hydrophobic value of −1.7 was obtained using this approach. For comparison, in hen egg white lysozyme, these values range from −7 to 1 for buried titratable residues, with the more positive values representing more hydrophobic contributions.

The electrostatic interaction between the oxidized dimer and a negatively charged amino acid residue can be described by Coulomb's law:

$$V = \frac{Q_1 Q_2}{4\pi\epsilon_0 r\epsilon}$$

where ϵ_0 is the permittivity of a vacuum. The energy of interaction (V) between the charges (Q_1 and Q_2) on the dimer and M199 is related to the difference of approximately 60 mV between the midpoint potential at low and high pH in the titration curve that is corrected for the wild-type dependence. With the Faraday constant = 1 meV/mV, an energy difference of 60 meV is assumed to be equivalent to the energy of interaction. The distance (r) can be approximated by the average distance between the conjugated atoms of the two bacteriochlorophylls of the dimer and the N and O atoms of Asn M199 in the wild-type structure. Assuming that Asp in the mutant is in the same position as Asn in the wild type, a value for r of approximately 14 Å is obtained. Substituting these values into Coulomb's law yields a dielectric constant for the medium (ϵ) of approximately 20.

The dielectric constant is difficult to measure experimentally. Previous estimates for the interior of proteins have been generally in the range of 10−20 (*23*−*26*). It should be noted that this is an average local effective dielectric constant, which is likely to be inhomogeneous throughout the protein, and it is not a microscopic constant (*27*, *28*). The shift of approximately 3 pH units in the pK_a value for Asp at M199 in the reaction center relative to its value in water, reflecting the free energy cost of burying a charged residue, is reasonable for a medium with a dielectric constant in this range (*19*). Thus, the magnitudes of both the change in energy of the dimer and the shift in the pK_a value for the aspartic acid residue are consistent with a relatively nonpolar local environment for the position of M199 and the dimer in the interior of the protein. Lower values within the range of 2.1−9.5 that have been estimated for the dielectric constant of the reaction center probably reflect the limited ability of the sample to respond to the presence of charges when the protein is in a glycerol and buffer glass at 1.5 K (*27*) compared to the buffer solution at room temperature used for these studies.

Further supporting the estimate of 20 for the dielectric constant is the observed additivity of the midpoint potential changes in the double and triple mutants. The additivity shows that the electrostatic interactions between the mutated residues and the dimer are independent, indicating that the charges of these residues are not highly interacting. One would not expect two charges separated by 25 Å in a medium with $\epsilon = 20$ to interact strongly. The introduction of Asp at L170 at the symmetry-related position resulted in a very similar change in the midpoint potential of the dimer compared to the introduction of Asp at M199, and in previous results, the substitution L166 Asn to Asp was shown to result in a slightly smaller difference in midpoint potential between low and high pH of 45 mV (*15*). The similarity in these values to those of M199 indicate a similar figure for the dielectric constant, although the pK_a values associated with the pH dependence of the change in midpoint potential in the L170 and L166 mutants were not determined.

The rate of charge recombination between the primary quinone acceptor and the dimer in wild type shows a slight increase with increasing pH, while in the M199 Asn to Asp mutant a distinct decrease in the rate is observed above pH 8 (Figure 3). In general, an increase in this rate should result from an increase in the free energy difference, with a relationship that can be described by Marcus theory. For wild type, the increase in rate from pH 6.5 to 9.5 is associated with a net increase of 35 meV in the free energy difference for this reaction, resulting from a combination of energetic changes in both the dimer and the quinone (*16*). For the M199 Asn to Asp mutant, the decrease in the rate at high pH likely results from a net decrease in the free energy difference corresponding to the decrease in the dimer midpoint potential.

Qualitatively the observed pH dependence of the charge recombination rate is consistent with the assumption that the energy of the charge-separated state changes as Asp M199 undergoes a change in ionization with pH. At low pH, this model would predict comparable rates rather than the approximate 2-fold lower rate for the mutant compared to wild type. This difference at low pH must arise from a difference either in the coupling or in the reorganization energy associated with the process. The coupling is probably not significantly altered, as the electronic factors that influence the coupling, such as the wave functions of the dimer, are not expected to be different in the mutant. However, the substitution of Asp for Asn in the environment of the dimer is likely to increase the reorganization energy. An increase in the reaction field energy would be expected for the introduction of an ionizable residue in a protein because of alterations that stabilize the neutral state of the residue, shifting the pK_a (*19*). This response in the nearby environment correspondingly should lead to an increase in the reorganization energy associated with oxidation of the dimer. For wild type, the free energy difference and reorganization energy for charge recombination are estimated to be approximately 500 and 900 meV, respectively (*10*). Assuming that other parameters are unchanged, a 100 meV increase in the reorganization energy for the mutant would

result in a 2-fold decrease in rate as observed. Thus, although other factors such as a change in coupling may contribute, the pH dependence of the rate for the mutant can be explained with a simple electrostatic model that includes an increase in the reorganization energy for the mutant compared to wild type.

In addition to the results presented here, electrostatic interactions have been modeled as having a significant impact on other electron-transfer rates of the reaction center. Large effects on initial electron-transfer rates have been shown to occur upon the introduction of a single ionizable residue near the active bacteriochlorophyll monomer (*29*). In this mutant, a pronounced alteration in the direction of electron transfer has been attributed to a proposed change in the energy of the monomer. The introduction of Asp or Lys near different chromophores of the reaction center also exerts an effect on electron-transfer rates (*30*, *31*). Residues near the secondary quinone have been shown to be ionizable and to affect the energies of the cofactors (*14*, *32*−*34*). The decrease in the energy of the charge-separated states shown in this work has consequences for a number of electron-transfer events in the reaction center. The effects on the rate and direction of the initial forward electron transfer will be described elsewhere (Haffa et al., manuscript in preparation).

ACKNOWLEDGMENT

We thank D. Smith and J. Dalsing for assistance with the preparation of the mutants.

REFERENCES

1. Michel-Beyerle, M. E., Plato, M., Deisenhofer, J., Michel, H., Bixon, M., and Jortner, J. (1988) *Biochim. Biophys. Acta 932*, 52−70.
2. Parson, W. W., Chu, Z. T., and Warshel, A. (1990) *Biochim. Biophys. Acta 1017*, 251−272.
3. Fajer, J., Hanson, L. K., Zerner, M. C., and Thompson, M. A. (1992) in *The Photosynthetic Bacterial Reaction Center II* (Breton, J., and Verméglio, A., Eds.) pp 33−42, Plenum Press, New York.
4. Marchi, M., Gehlen, J. N., Chandler, D., and Newton, M. (1993) *J. Am. Chem. Soc. 115*, 4178−4190.
5. Alden, R. G., Parson, W. W., Chu, Z. T., and Warshel, A. (1995) *J. Am. Chem. Soc. 117*, 12284−12298.
6. Gunner, M. R., Nicholls, A., and Honig, B. (1996) *J. Phys. Chem. 100*, 4277−4291.
7. Allen, J. P., and Williams, J. C. (1995) *J. Bioenerg. Biomembr. 27*, 275−283.
8. Gunner, M. R., and Honig, B. (1992) in *The Photosynthetic Bacterial Reaction Center II* (Breton, J., and Verméglio, A., Eds.) pp 403−410, Plenum Press, New York.
9. Beroza, P., Fredkin, D. R., Okamura, M. Y., and Feher, G. (1995) *Biophys. J. 68*, 2233−2250.
10. Lin, X., Murchison, H. A., Nagarajan, V., Parson, W. W., Allen, J. P., and Williams, J. C. (1994) *Proc. Natl. Acad. Sci. U.S.A. 91*, 10265−10269.
11. Goldsmith, J. O., and Boxer, S. G. (1996) *Biochim. Biophys. Acta 1276*, 171−175.
12. Kleinherenbrink, F. A. M., Chiou, H. C., LoBrutto, R., and Blankenship, R. E. (1994) *Photosynth. Res. 41*, 115−123.
13. Murchison, H. A., Alden, R. G., Allen, J. P., Peloquin, J. M., Taguchi, A. K. W., Woodbury, N. W., and Williams, J. C. (1993) *Biochemistry 32*, 3498−3505.
14. Maróti, P., Hanson, D. K., Baciou, L., Schiffer, M., and Sebban, P. (1994) *Proc. Natl. Acad. Sci. U.S.A. 91*, 5617−5621.
15. Ivancich, A., Mattioli, T. A., Artz, K., Wang, S., Allen, J. P., and Williams, J. C. (1997) *Biochemistry 36*, 3027−3036.
16. Feher, G., Arno, T. R., and Okamura, M. Y. (1988) in *The Photosynthetic Bacterial Reaction Center II* (Breton, J., and Verméglio, A., Eds.) pp 271−287, Plenum Press, New York.
17. Mattioli, T. A., Lin, X., Allen, J. P., and Williams, J. C. (1995) *Biochemistry 34*, 6142−6152.
18. Honig, B., and Nicholls, A. (1995) *Science 268*, 1144−1149.
19. Gunner, M. R., and Alexov, E. (2000) *Biochim. Biophys. Acta 1458*, 63−87.
20. Dwyer, J. J., Gittis, A. G., Karp, D. A., Lattman, E. E., Spencer, D. S., Stites, W. E., and García-Moreno, E. B. (2000) *Biophys. J. 79*, 1610−1620.
21. Wilson, N. A., Barbar, E., Fuchs, J. A., and Woodward, C. (1995) *Biochemistry 34*, 8931−8939.
22. Mehler, E. L., and Guarnieri, F. (1999) *Biophys. J. 75*, 3−22.
23. Antosiewicz, J., McCammon, J. A., and Gilson, M. K. (1994) *J. Mol. Biol. 238*, 415−436.
24. Mauzerall, D. C., Gunner, M. R., and Zhang, J. W. (1995) *Biophys. J. 68*, 275−280.
25. Simonson, T., and Perahia, D. (1995) *Proc. Natl. Acad. Sci. U.S.A. 92*, 1082−1086.
26. Demchuk, E., and Wade, R. C. (1996) *J. Phys. Chem. 100*, 17373−17387.
27. Steffen, M. A., Lao, K., and Boxer, S. G. (1994) *Science 264*, 810−816.
28. Warshel, A., and Papazyan, A. (1998) *Curr. Opin. Struct. Biol. 8*, 211−217.
29. Heller, B. A., Holten, D., and Kirmaier, C. (1995) *Science 269*, 940−945.
30. Heller, B. A., Holten, D., and Kirmaier, C. (1996) *Biochemistry 35*, 15418−15427.
31. Kirmaier, C., Weems, D., and Holten, D. (1999) *Biochemistry 38*, 11516−11530.
32. Takahashi, E., and Wraight, C. A. (1992) *Biochemistry 31*, 855−866.
33. Lancaster, C. R. D., Michel, H., Honig, B., and Gunner, M. R. (1996) *Biophys. J. 70*, 2469−2492.
34. Paddock, M. L., Feher, G., and Okamura, M. Y. (1997) *Biochemistry 36*, 14238−14249.

BI011574Z